Synthesis and catalytic reactivity of MCM-22/ZSM-35 composites for olefin aromatization

Xionglei Niu[a], Yueqing Song[a], Sujuan Xie[a], Shenglin Liu[a], Qingxia Wang[a], and Longya Xu[a,*]

State Key Laboratory of Catalysis, Dalian Institute of Chemical Physics, Chinese Academy of Sciences, Dalian, P.O. Box 110, 116023, P. R. China

A series of MCM-22/ZSM-35 composites has been hydrothermally synthesized and characterized by XRD, SEM, particle size distribution analysis, N_2 adsorption and NH_3-TPD techniques. Pulse and continuous flow reactions were carried out to evaluate the catalytic performances of these composites in aromatization of olefins, respectively. It was found that MCM-22/ZSM-35 composites could be rapidly crystallized at 174 °C with an optimal gel composition of $SiO_2/Al_2O_3 = 25$, $Na_2O/SiO_2 = 0.11$, $HMI/SiO_2 = 0.35$, and $H_2O/SiO_2 = 45$ (molar ratio), of which the weight ratio of ZSM-35 zeolite in the composite relied on the crystallization time. The coexistence of MCM-22 and ZSM-35 in the composite (MCM-22/ZSM-35 = 45/55 wt/wt) was observed to exert a notable synergistic effect on the aromatization ability for butene conversion and FCC gasoline updating, possibly due to the intergrowth of some MCM-22 and ZSM-35 layers.

KEY WORDS: MCM-22/ZSM-35 composites; synthesis; aromatization; olefin.

1. Introduction

Nowadays, micro-porous and meso-porous materials have been highlighted by their huge industrial and commercial values [1, 2]. Zeolites, in particular alumina-silicate zeolites as archetypal micro-porous materials, have found a wide use in the area of catalysis as catalysts, supports, adsorbents and ion exchangers etc. Generally, zeolites with a single structure are directly applied; however, in some cases mixed or composite zeolites are preferred due to the exhibition of a special performance. For instance, ZSM-5/ZSM-11 composite, a co-crystalline zeolite [3, 4], showed a high activity, selectivity and stability for the alkylation reaction of benzene with the dilute ethylene in FCC off gas, and ZSM-5/ZSM-11 intermediate [5, 6] effectively catalyzed the conversion of methanol and the alkylation of aromatics. ZSM-5/Y composites consisting of either the mechanical mixture of ZSM-5 and Y [7] or the *in-situ* synthesized ZSM-5/Y composites [8] were reported to exhibit a notable synergy in the catalysis. Recently, the synthesis of some microporous/mesoporous composites, such as ZSM-5/MCM-41, Beta/MCM-41, Y/MCM-41 and Ti-Beta/SBA-15, has aroused great interest in the catalytic applications, as they can combine the advantages of microporous materials with high activity and stability and mesoporous materials with large pore size [9].

Although Mobil Corporation first reported the synthesis of laminar MCM-22 zeolite in 1990 [10], until in 1994 the elucidation of the structure was just completed [11]. MCM-22 [11] is constituted of two non-intersecting pore systems, i.e. a two-dimensional sinusoidal 10-membered ring (MR) pore channel (0.40 nm×0.59 nm) and a 12-MR supercage (0.71 nm×0.71 nm×1.82 nm) connected by a one-dimensional 10-MR pore channel. Furthermore, it is featured by a thin-plate morphology with a large quantity of super-cage pockets on the external surface of the crystal, as well as a special acidity distribution, both in channel and on the surface. Up to date, MCM-22 zeolite has been extensively applied in many heterogeneous catalytic reactions, inclusive of gasoline upgrading, fluidized catalytic cracking, alkylation of aromatics and isomerization and aromatization of hydrocarbons [12].

Much effort has been paid to the synthesis of MCM-22 [13–15], and the post-synthesis treatment led to delaminated ITQ-2 zeolite [16]. Due to the metastable characteristics, MCM–22 tends to accompany with other zeolites like ZSM-5, ZSM-35 etc. [14]. Recently, Mochida *et al*. [15] studied the effect of Si/Al ratio on the crystallization of MCM-22 under certain temperatures, and claimed the easy transformation of MCM-22 into ZSM-35 with excess time. Likewise, ZSM-35 zeolite also possesses laminar morphology, and can be delaminated to ITQ-6 zeolite [17]. ZSM-35 belongs to the FER topology, consisting of two-dimensional intersecting channel system, namely 10-MR (0.54 nm×0.42 nm) channel and 8-MR (0.35 nm) channel, parallel to [001] and [010] directions, respectively [18]. It has been widely applied in catalytic processes, such as the cracking of hydrocarbons and the skeletal isomerization of *n*-olefins to *iso*-olefins [19].

---

* To whom correspondence should be addressed.
  E-mail: lyxu@dicp.ac.cn

Previously, we concentrated our effort on the synthesis and catalytic application of MCM-22 for methane dehydroaromatization [20]. It has been found that MCM-22 could be a stable support for methane dehydroaromatization owing to its special acidic character and pore-channel structure as well as its high coke deposition capacity [20]. In this paper, we will present the investigation of the effect of synthesis factor on the MCM-22/ZSM-35 composites, and their catalytic performance for the butene/liquefied petroleum gas (LPG) /FCC gasoline aromatization. For the MCM-22/ZSM-35 composites synthesized with various ratios of MCM-22 to ZSM-35 zeolite, some interesting information has been achieved that their physical properties and acidities, as well as their catalytic activities, are quite different from that of MCM-22/ZSM-35 mechanical mixture.

2. Experimental

2.1. Synthesis of MCM-22/ZSM-35 composites

The raw materials used were silica sol (26.6 wt. % SiO_2, China medicine (group) shanghai chemical reagent Co.), sodium aluminate (43.0 wt. % Al_2O_3, 51.5 wt % Na_2O, China medicine (group) shanghai chemical reagent Co.), hexamethyleneimine (HMI) (98 wt.%, Acros Organics), and de-ionized water. Sodium aluminate was dissolved in de-ionized water, followed by the addition of sodium hydroxide solution (0.10 g/ml), HMI (as structure-directing agent), and silica sol under vigorous stirring, resulting in the final mixture with a molar composition of $Na_2O/SiO_2 = 0.11$, $HMI/SiO_2 = 0.35$, $H_2O/SiO_2 = 45$, $SiO_2/Al_2O_3 = 20$–50. Then, the precursor suspension was transferred into a stainless steel autoclave, where the crystallization was performed dynamically at 60 rpm at given temperatures. After the completion of crystallization, the autoclave was quenched by tap water. Subsequently, the solid product was recovered centrifugally (5000 rpm) and washed several times with de-ionized water till pH = 7–8. Then the samples were dried at 110 °C for 8 h. A series of samples with SiO_2/Al_2O_3 ratio of 25 crystallized at 174 °C for 60, 76, 84, 90, 96, 108 and 120 h, were denoted as A–G, respectively.

2.2. Preparation of catalysts

For catalysts used in the pulse reaction of butene aromatization, the above-mentioned zeolite samples of A, B, D, E and G were first removed organic templates by calcination at 550 °C for 5 h, and then ion-exchanged as follows: The Na-type solids were ion-exchanged with an aqueous NH_4NO_3 solution (0.8 M) three times into NH_4^+-type zeolites. Each time, 1 g of the solid was treated with 12 ml of NH_4NO_3 solution at 80 °C for 2 h under stirring, in which the pH of the mixture was kept at ~8 by adjustment with NH_4OH. Then the resulting NH_4^+-form of the zeolites were calcined again at 520 °C for 2 h in air to form the H-type zeolites, followed by pressing, crushing and sieving into 30–40 mesh catalysts. These catalysts achieved were denoted as cat-A, cat-B, cat-D, cat-E and cat-G, respectively. As a reference, cat-M was prepared from a mechanical mixture of zeolite samples A and G, with a weight ratio of 45:55.

As for catalysts used in continuous reactions of LPG/FCC gasoline aromatization, selected as-made zeolite samples of A, B, D, E and G were first mixed with alumina according to the weight ratio of 70:30 in the presence of dilute nitric acid, pressed into extrudes (ϕ 1.6 mm), dried at 120 °C, calcined at 550 °C and then followed by the same steps mentioned-above, i.e. ion-exchange, calcination, crushing and sieving into 20–40 mesh particle catalysts. These catalysts were represented by cat-AB, cat-BB, cat-DB, cat-EB and cat-GB. As a comparison, cat-MB was prepared from a mechanical mixture of zeolite samples A and G with a weight ratio of 45:55 using 30 wt.% of alumina. It is noted that the alumina acts as a binder to increase the strength of the catalysts for the LPG/FCC gasoline aromatization reaction and its reactive performance is negligible under the reaction conditions.

2.3. Characterization of samples

XRD. XRD patterns of the calcined samples were recorded on a Rigaku D/max-rb diffractometer with Ni-filtered Cu Kα radiation scanned in the 2θ range of 5–40°. The content of ZSM-35 in the composite of MCM-22/ZSM-35 was determined by the internal standard method using fluorite as the reference [21].

Particle Size Distribution. The particle size was measured on a Betersizer (China) equipped with a laser-detector. First the above-mentioned wet samples (already washed to pH = 7–8) were re-dispersed in de-ionized water with the assistance of ultrasonic to form a uniform 'solution'. After the background was taken, drops of the 'solution' were added to a quartz cell half filled with de-ionized water till a favorable concentration was achieved. Then the laser signals were recorded and PSD-calculations were done by the computer according to Reyleigh theory. The repetition errors of measurements are within 2%.

SEM. Scanning electron microscopy (SEM) was performed on a Hitachi-600 scanning electron microscope operating at an accelerating voltage of 25 kV.

N$_2$ adsorption. Micromeretics ASAP-2010 system was used to determine the N_2 adsorption–desorption isotherms of the samples at −196 °C. The BET specific surface area was calculated in terms of the Brunauer-Emmett-Teller (BET) equation. The pore size distribution was estimated by the Horvath-Kawazoe (HK) method. Prior to the measurements, the samples were degassed at 350 °C for 2 h.

NH₃ temperature programmed desorption (NH₃-TPD). NH₃-TPD measurements were carried out in a conventional U-shaped stainless-steel micro-reactor (i.d. = 4 mm) using flowing helium (He) as the carrier gas. An on-line gas chromatograph (GC) equipped with a TCD detector monitored the NH₃-TPD process. A detailed procedure was described below: after the sample (0.140 g) was pretreated at 600 °C for 30 min in the flow of helium (25 ml/min), it was cooled down to 150 °C, and followed by the saturation with a He stream containing NH₃ for 10 min; then the sample was purged with the flow of helium for some time until a stable GC-baseline was attained. Finally, NH₃-TPD process was carried out in the range of 150–600 °C at a heating rate of 18.8 °C/min.

2.4. Catalysts test

2.4.1. Catalytic performance of MCM-22/ZSM-35 composites for the aromatization of butene in the pulse reaction mode

The pulse reaction was performed under atmospheric pressure in a stainless micro-reactor (i.d = 3 mm, packed with 0.2 g catalyst) with an injection port. Nitrogen was used as carrier gas (flow rate = 20 cm³ min⁻¹). After the catalyst was pretreated at 500 °C for 0.5 h in nitrogen and cooled down to the reaction temperature (350 °C), a feeding dose of about 0.05 mmol butene was injected into the micro-reactor. The products formed were directly detected by an on-line Omnistar mass spectrumeter (Blazer Corp, Switzerland).

2.4.2. Catalytic performance of MCM-22/ZSM-35 composites for the aromatization of olefin in LPG in the continuous reaction mode

Continuous flow reactions were conducted in a stainless-steel fixed-bed reactor (i.d. 11 mm), loaded with 4.0 g of the catalyst, operating at 400 °C under the pressure of 0.5 MPa with the feed gas consisting of the liquefied petroleum gas (propane 4.22 wt%, n-butane 10.13 wt%, iso-butane 43.74 wt%, 1-butene 17.2 wt%, trans-2-butene 15.12 wt%, cis-2-butene 9.59 wt%). Note that the catalyst had been pretreated at 500 °C for 1 h in the flow of nitrogen before the feed gas was pumped into the reactor with a space velocity of WSHV = 2 h⁻¹. Each reaction reached stable state within 2 h of reaction; the liquid and gas products were then analyzed on stream by flame ion detector (FID) and thermal conductivity detector (TCD) installed on a Varian-3800 gas chromatograph, respectively.

2.4.3. Catalytic performance of MCM-22/ZSM-35 composites for FCC gasoline upgrading in the continuous reaction mode

FCC gasoline upgrading reaction was carried out in a micro-reactor (16 mm i.d.). After 7.0 g of catalyst was loaded, the reactor was heated from room temperature to 500 °C at a rate of 200 °C/h in a flow of hydrogen,

then maintained at 500 °C for 1 h. After that, it was cooled to the reaction temperature of 250 °C. Then, the mixture feed of hydrogen and gasoline with a ratio of 400:1 (V/V) was passed through the reactor instead of hydrogen. The tail gas was analyzed by an on-line gas chromatography equipped with a 9-m squalane column and a thermal conductivity detector (TCD), while the liquid product was analyzed by a Varian 3800 gas chromatography with a 100-m pona capillary column and a flame ionization detector (FID).

3. Results and discussions

3.1. Optimizations of temperature and SiO_2/Al_2O_3 ratio for the synthesis of MCM-22/ZSM-35 composites

In general, MCM-22 was hydrothermally synthesized at about 150 °C with a gel composition of 30 SiO_2: 1 Al_2O_3: 3.3 Na_2O: 10.5 HMI: 1350 H_2O (molar ratio) [13, 14], while a relative high temperature usually caused the transformation of crystalline phase to ZSM-35, which is more thermodynamically stable. With other synthetic parameters being constant, the synthesis temperature and silica to alumina ratio are crucial factors for the forming of a specific type of zeolite.

Table 1 presents the effect of some synthesis parameters on the crystallization. When the SiO_2/Al_2O_3 ratio was not less than 40, a mixed phase of ZSM-35 and tridymite was formed at 166 °C in the period from 90 to 108 h. Decreasing the SiO_2/Al_2O_3 ratio to a certain value between 20 and 30, MCM-22 could be crystallized as a pure phase within 108 h. These results allow us to focus on SiO_2/Al_2O_3 ratio not higher than 30 in the following synthesis screening for appropriate temperature for synthesis of MCM-22/ZSM-35 composites.

Table 1
Optimization of synthesis conditions with a fixed gel composition of $Na_2O/SiO_2 = 0.11$, $H_2O/SiO_2 = 45$, $HMI/SiO_2 = 0.35$

Entry	SiO_2/Al_2O_3	Tempt. (°C)	Time (h)	Zeolite type
1	20	166	90	MCM-22
2	20	166	108	MCM-22
3	30	166	90	MCM-22
4	30	166	108	MCM-22
5	40	166	90	ZSM-35/tridymite
6	40	166	108	ZSM-35/tridymite
7	50	166	90	ZSM-35/tridymite
8	50	166	108	ZSM-35/tridymite
9	20	178	90	ZSM-35
10	30	178	90	MCM-22/ZSM-35/tridymite
11	30	174	90	MCM-22/ZSM-35/tridymite
12	25	174	90	MCM-22/ZSM-35
13	20	174	90	MCM-22/ZSM-35

When the temperature was elevated to 178 °C, MCM-22/ZSM-35/tridymite was always obtained. However, a small drop of temperature to 174 °C significantly reduced the percentage of tridymite phase when SiO_2/Al_2O_3 is 30 (quantitative data are not shown here). MCM-22/ZSM-35 composites were observed to form at 174 °C in 90 h with a gel composition of $SiO_2/Al_2O_3 = 25$, $Na_2O/SiO_2 = 0.11$, $H_2O/SiO_2 = 45$ and $HMI/SiO2 = 0.35$.

Based on these results, the temperature of 174 °C and $SiO_2/Al_2O_3 = 25$, $Na_2O/SiO_2 = 0.11$, $H_2O/SiO_2 = 45$ and $HMI/SiO_2 = 0.35$, are regarded as suitable conditions for the synthesis of MCM-22/ZSM-35 composites in this paper.

3.2. The effect of crystallization time on the synthesis of MCM-22/ZSM-35 composites

Under the favorable conditions mentioned above, a series of MCM-22/ZSM-35 composites were obtained with various contents of ZSM-35 by varying synthesis time from 60 to 120 h. The effect of the crystallization time on the transformation of crystalline phases of these samples has been confirmed by XRD patterns (Figure 1). Very distinctly, the formation of pure MCM-22 and ZSM-35 phases occurred at crystallization time of 60 and 120 h, respectively, while crystallization period between 60 and 120 h led to MCM-22/ZSM-35 composites. As depicted in figure 2, the percentage of ZSM-35 in MCM-22/ZSM-35 composites varied with the crystallization time on stream. It is evident that the transformation of MCM-22 to ZSM-35 was accelerated in the range of 76–96 h. SEM images of samples A and G (in figure 3) clearly show that these materials are composed of well-crystallized laminar plates with a mean size of around 2.2 μm.

Figure 2 also shows the mean particle size of samples varied with the crystallization time. It has a slight increase when the crystallization time was prolonged from 76 to 96 h, and then keeps nearly constant (about 2.4 μm, which is comparable to the data obtained by SEM). These results suggest that the dissolution of laminar crystals of MCM-22 did not take place during the transformation, and the transformation of MCM-22 to ZSM-35 could follow a solid-to-solid mechanism, as described elsewhere [22]. The driving force of transformation may derive from a relative high stability of the sub-unit linkage mode or channel system of ZSM-35 than MCM-22 as discussed by Peng et al. [23].

3.3. The characterization of MCM-22/ZSM-35 composites by N2 physisorption and NH3-TPD

Table 2 shows some pore properties of MCM-22/ZSM-35 composites. It is clear that the largest mean pore size and the smallest one are 5.32 Å for MCM-22 (sample A) and 4.86 Å for ZSM-35 (sample G), respectively. Based on these values, the calculated values of the average pore size for the mechanical mixture of MCM-22 and ZSM-35 zeolite should decrease with ZSM-35 content increasing, which is quite similar to the experimental data. For the synthesized MCM-22/ZSM-35 composites, as can be observed from Table 2, their mean pore size show the same decreasing tendency with more and more ZSM-35 content in MCM-22/ZSM-35 composites.

As for the specific surface area of these samples, MCM-22 (sample A) has a BET surface area of 398 m^2/g, much larger than that of ZSM-35 (280.3 m^2/g). For the mechanical mixture of MCM-22/ZSM-35 with various ZSM-35 content, their BET surface areas will decrease accordingly with ZSM-35 content as being indicated in Table 2. However, the change tendency of BET surface area for the synthesized MCM-22/ZSM-35 composites disagrees with that mentioned above. Especially, sample D (MCM-22/ZSM-35
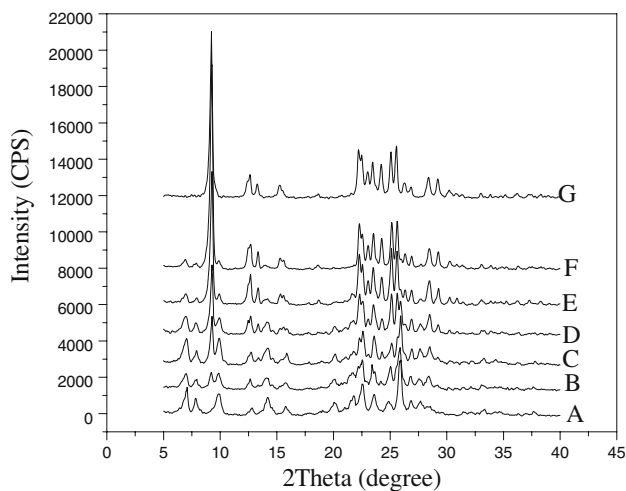

Figure 1. XRD patterns of calcined samples (A: 60 h, B: 76 h, C: 84 h, D: 90 h, E: 96 h, F: 108 h, G: 120 h).
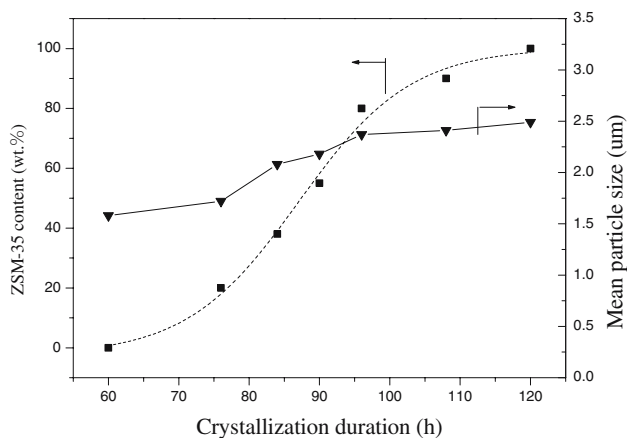

Figure 2. ZSM-35 contents and mean particle size of samples against crystallization duration.
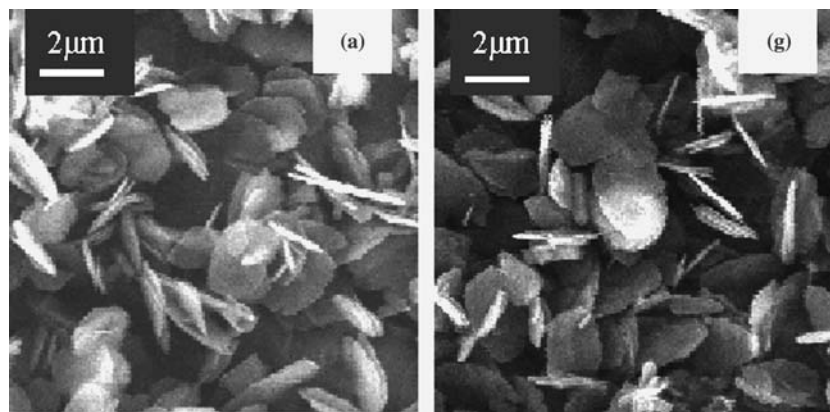
Figure 3. Representative SEM images of as-made samples (A: MCM-22; G: ZSM-35).

Table 2
Pore properties of zeolite sample obtained from N_2 adsorption iso-thermal

Sample	MCM-22: SM-35 Wt./wt.)	BET (m^2/g)	Mean pore size (Å)
A	100: 0	398.1	5.32
B	80: 20	385.1(374.5) *	5.17(5.23) *
D	45: 55	405.8(333.1)	5.17(5.07)
E	20: 80	281.8(303.9)	4.96(4.95)
G	0: 100	280.3	4.86

*: The value in parentheses is calculated according to respective percentage contribution of MCM-22 and ZSM-35.

composites with 55-wt% of ZSM-35) has a BET surface area of 405.8 m^2/g, which is much larger than 333.3 m^2/g of the mechanical mixture of MCM-22/ZSM-35. This implies that these-synthesized MCM-22/ZSM-35 composites are not separate crystal mechanical mixture of MCM-22 and ZSM-35, but may be constituted of some intergrowth of MCM-22 and ZSM-35 layers.

Besides the increment in the BET specific surface areas for the synthesized MCM-22/ZSM-35 composites, the acidity of these samples exhibits some specialties with increasing ZSM-35 content. The NH_3-TPD profiles in figure 4 show that both weak acid sites (between the desorption temperature of 250 °C and 350 °C) and strong acid sites (between the desorption temperature of 450 and 600 °C) coexist on the surface of these samples, and pure ZSM-35 zeolite has much more acid sites than that on pure MCM-22 zeolite. It is reasonable that the MCM-22/ZSM-35 composites have more acid sites, both in weak and strong ones, with the increase of ZSM-35 (as shown in Table 3). However, there is some difference between the acidity of the MCM-22/ZSM-35 mechanical mixtures and the synthesized MCM-22/ZSM-35 composites. For example, sample M, as a mechanical mixture of MCM-22/ZSM-35, has more acid sites than its synthesized counterpart (sample D). These results also indicate that the synthesized MCM-22/ZSM-35 composites are not separate crystal mixture of MCM-22 and ZSM-35.
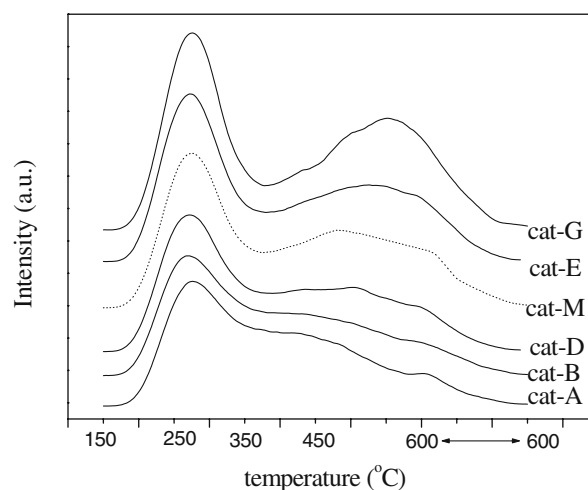
Figure 4. NH_3 – TPD curves of samples.

3.4. Catalytic performance of MCM-22/ZSM-35 composites for the aromatization of butene in the pulse reaction mode

In order to access the catalytic performance of the MCM-22/ZSM-35 composite catalysts, pulse reactions have been carried out to study the initial activity of butene aromatization with the products formed directly detected by an on-line multi-channel MAS. Here, mass to charge ratio (M/e) of 78, 91, 92, 106 and 120 denote to benzene, non-benzene aromatics, toluene, C_8 aromatics and C_9 aromatics, respectively [24, 25], and the ion abundance (or the peak area) represents the relative amount of aromatics formed. For simplification, M/e = 91, corresponding to non-benzene aromatics, were selected as an indicative of catalytic activity [24].

The intensity of M/e 91 against duration is depicted in figure 5. Supposed that the peak area of pure MCM-22 catalyst is unit, the relative ratios of peak area for cat-A: cat-B: cat-D: cat-E: cat-G is 1.0: 0.96: 4.0: 0.99: 0.1. That is to say, pure MCM-22 (cat-A) shows promising aromatization performance, which is much higher than

Table 3
Acid sites distribution information obtained from NH$_3$-TPD measurements

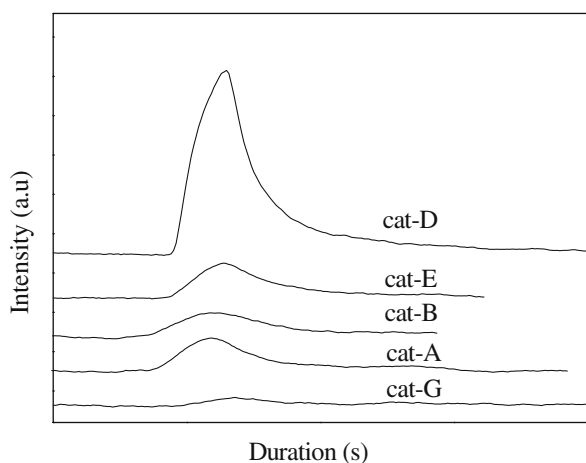| Sample	Weak acid sites (mmol/g)	Strong acid sites (mmol/g)
A	132.8	134.5
B	134.5	149.4
D/M	147.8/157.7	146.1/159.4
E	169.4	161.0
G	192.6	194.3

Figure 5. Performances of butene aromatization on various catalysts.

that of pure ZSM-35 (cat-G). To our surprise, the synthesized MCM-22/ZSM-35 composite catalysts (cat-B, cat-D and cat-E) show relative higher aromatization ability. Especially for cat-D with MCM-22/ZSM-35 weight ratio of 45–55, its reactivity is up to about 4 times that of the pure MCM-22 catalyst. Although the further catalytic reaction mechanism is underway, the advantage of the synthesized MCM-22/ZSM-35 composite over catalysts from the pure MCM-22 and ZSM-35 zeolite is a very interesting phenomenon. Currently, we propose that the intergrowths of MCM-22 and ZSM-35 layers

result in some synergy effect of MCM-22 and ZSM-35 in butene aromatization process, and an optimum MCM-22 to ZSM-35 ratio seems to exist for transformation of butene to aromatics.

3.5. Catalytic performance of MCM-22/ZSM-35 composites for the aromatization performance of LPG in the continuous flow reaction mode

LPG constituting of mainly butane and butene, was usually consumed as household fuel. With the success of West-to-East Gas Transmission Project in China, more LPG will seek for new usage. It may be a better option that under relative low temperature butene in LPG is transformed to aromatics as high RON (Research Octane Number) gasoline additive. Thus, the aromatization reaction of LPG was selected to examine the catalytic performance of MCM-22/ZSM-35 zeolites mentioned above.

Under the reaction conditions of 400 °C, 0.5 MPa and WHSV 2 h^{-1}, butene-in-LPG (liquefied petroleum gas feed) can be converted to aromatics, as being demonstrated in Table 4. From the reaction results, it can be observed that the conversion of butene reaches as high as 99.44% over pure MCM-22 (cat-AB), 80.50% over ZSM-35 (cat-GB). As for MCM-22/ZSM-35 composite catalysts, the conversion of butene over cat-BB and cat-DB are similar to that of MCM-22, while the conversion of butene over cat-EB is close to that over ZSM-35. With regard to the aromatization performance, MCM-22 shows very good aromatic selectivity of 64.25 wt.%, while ZSM-35 does poorly, with only 24.58 wt.% of aromatics selectivity. It is clear that, for the synthesized MCM-22/ZSM-35 composites catalyst, their aromatization performances were to decrease with increase of ZSM-35 content on the whole, except for the catalyst of cat-BB. Its aromatic selectivity is 67.74 wt.%, which is about 2.5 wt.% higher than that of pure MCM-22. This behavior can also be contributed to the synergy effect of MCM-22 and ZSM-35 layers.

Table 4
Comparison of the catalytic activity of various catalysts

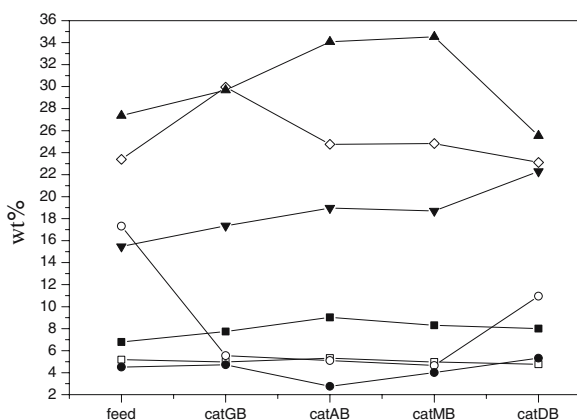| Catalyst	cat-AB	cat-BB	cat–DB	cat-EB	cat-GB
MCM-22: ZSM-35 (wt./wt.)	100:0	80:20	45:55	20:80fs	0:100
Olefin conversion (%)	99.44%	98.32%	98.67%	84.96%	80.50%
Liquid product distribution (wt.%)					
n-paraffins	7.59	6.36	8.61	10.66	4.47
iso-paraffins	20.07	15.04	20.53	19.15	13.96
cyclo-paraffins	1.87	2.01	3.74	6.44	5.50
Olefins	1.51	1.87	2.99	8.21	42.20
aromatics	65.25	67.74	53.19	48.47	24.58
LCO	4.67	6.97	10.91	7.07	9.29

Reaction temperature 400 °C, P = 0.5 MPa , WHSV = 2 h^{-1}.

3.6. The performance of MCM-22/ZSM-35 composites catalyst for FCC gasoline upgrading

In China about 80% gasoline used is produced through the FCC (Fluid Catalytic Cracking) process, which contains about 50% olefins on average [26]. The content of olefin is too high to satisfy the regulation that is newly issued on the composition of gasoline [26]. Based on the results discussed in section 3.4 and 3.5, isomerization and aromatization reactions of olefins in gasoline, which could maintain or increase the RON of gasoline accompanying the decrease of olefin, may be a wise way. Here some MCM-22/ZSM-35 catalysts were used for the FCC gasoline upgrade, and some desirable improvements for the FCC gasoline quality have been achieved (Figure 6). In this catalytic process, discussions will be concentrated on the iso-paraffins and aromatics contents variation, which has very close relationship with RON of gasoline.

From the data shown in figure 6, the content of iso-paraffin relative to feed is found to increase by 6.7, 2.31, and 7.16 wt.% over pure MCM-22 (cat-AB), ZSM-35 catalysts (cat-GB) and MCM-22/ZSM-35 mechanical mixture catalyst (cat-MB), respectively. Quite surprisingly, cat-DB, as a synthesized counterpart of cat-MB, exhibits a small drop of iso-paraffins (by 1.83 wt.%) relative to feed. With respect to the content of aromatics, it is enhanced over all the catalysts, i.e. by 3.5, 1.89, and 3.24 wt.% over MCM-22, ZSM-35 and cat-MB, respectively. Especially, the aromatic content over cat-DB from a synthesized MCM-22/ZSM-35 composite with weight ratio of 45–55 can reach as much as 22.5 wt.%, which is about 6.8 wt.% higher than that in the feed.

Another observation from figure 6 is that more branched olefins can be yielded over pure ZSM-35 catalyst (cat-GB) during the reaction, indicating that the hydrocarbon derived from unbranched olefins tend to take skeletal isomerization due to the relative small channel space of ZSM-35 (10- and 8-MR). It is reported that the hydrogen transfer reaction can occur between dimerized products from activated alkenes and other hydrocarbons in the cavities located in the intersection of 10-MR channel [27, 28]. Considering the larger pore size of MCM-22 (12- and 10-MR) and its special acidity, it is reasonable that such enough space would enable carbonium ion to take the inter-molecular hydrogen transfer reaction more easily. So the iso-paraffins and aromatics are more easily formed on the pure MCM-22 zeolite catalyst than on the pure ZSM-35 zeolite catalyst. For the high aromatization performance of cat-DB, it is temporally assumed that the iso-paraffins and/or branched olefins formed on ZSM-35 layers of the MCM-22/ZSM-35 intergrowth may be consumed as intermediates for the aromatics formed on MCM-22 layers, as a result, not higher iso-paraffin but the highest aromatics selectivity is produced on the MCM-22/ZSM-35 composites.

4. Conclusions

This work can be summarized as follows:

(1) A series of MCM-22/ZSM-35 composites could be synthesized successfully with rather short synthesis time under conditions of 174 °C, SAR = 25, $Na_2O/SiO_2 = 0.11$, $HMI/SiO_2 = 0.35$, and $H_2O/SiO_2 = 45$. These composites could be constituted of some intergrowth of MCM-22 and ZSM-35 layers.

(2) Among the catalysts of MCM-22/ZSM-35 series for the butene aromatization reactions in pulse mode, the synthesized MCM-22/ZSM-35 composite with a MCM-22/ZSM-35 ratio of 45/45 (wt/wt) exhibit a maximum of aromatization performance.

(3) With regard to their catalytic performance for the aromatization of olefins in LPG/FCC gasoline, the synthesized MCM-22/ZSM-35 composite catalyst could show higher aromatization activity than pure MCM-22 or pure ZSM-35 zeolite catalyst, possibly due to the synergism of ZSM-35 and MCM-22 zeolites.

Figure 6. Comparison of products distribution of the feed gasoline and gasoline reacted on different catalysts (reaction temperature: 250 °C, pressure: 0.4 Mpa, WHSV: 1.0 h^{-1}, H$_2$/gasoline: 400 (v/v), time on stream: 2 h, reaction mode: continuous).

Symbol specification: ■: cyclo-paraffin; □: n-paraffin; ▲: iso-paraffin; ▼: aromatics; ◇: branched-olefin; ○: unbranched-olefin; ●: cyclo-olefin.

References

[1] S.I. Zones and M.E. Davis, Curr. Opin. Solid State Mater. Chem. 1 (1996) 107.

[2] A.K. Cheetham, G. Ferey and T. Loiseau, Angew. Chem. Int. Ed. Engl. 38 (1999) 3268.

[3] Q.X. Wang, S.R. Zhang, G.Y. Cai, F. Li, L.Y. Xu, Z.X. Huang and Y.Y. Li, US Patent 5,869,021 (1999).

[4] Q.X. Wang, S.R. Zhang, G.Y. Cai, F. Li, L.Y. Xu, Z.X. Huang and Y.Y. Li, US Patent 6,093,866 (2000).

[5] G.T. Kokotailo, US Patent 4,229,424 (1980).

[6] G.T. Kokotailo, US Patent 4,289,607 (1981).

[7] (a) I.P. Dzkih, J.M. Lopes, F. Lemos and F. Ramoa Ribeiro, Appl. Catal., A , 176 (1999) 239; (b) I.P. Dzkih, J.M. Lopes, F. Lemos and F. Ramoa Ribeiro, Catal. Today 65 (2001) 143.

[8] H.L. Chen, B.J. Shen and H.F. Pan, Chem. Lett. 32 (2003) 726.

[9] Y. Han and F.S. Xiao, Chin. J. Catal. 24 (2003) 149.

[10] M.K. Rubin and P. Chu, US Patent 4,954,325 (1990).

[11] M.F. Leonowicz, J.A. Lawton, S.L. Lawton and M.K. Rubin, Science 264 (1994) 1910.

[12] (a) Del, Rossi Kenneth J.; Huss, Albin, US Patent 5,107,047 (1992); (b) J.E. Child, A. Huss Jr., F.J. Krambeck, F.P. Ragonese, R.T. Thomson and S. Yurchak, US Patent 5,073,665 (1991); (c) Absil, Robert P.L.; Bowes, US Patent 5,085,762 (1992).

[13] (a) I. Güray, J. Warzywoda, N. Bac, et al., Micro. Meso. Mater. 31 (1999) 241; (b) R. Aiello, F. Crea, F. Testa, et al., Micro. Meso. Mater. 35–36 (2000) 585; (c) M. Cheng, D. Tan, X. Liu et al., Micro. Meso. Mater. 42 (2001) 307.

[14] (a) R. Ravishankar, Tapas Sen, Stud. Surf. Sci. Catal. 84 (1994) 331; (b) A. Corma, C. Corell, Zeolites 15 (1995) 2; (c) Ana Lucia antos Marques, Micro. Meso. Mater. 32 (1999) 131.

[15] I. Mochida, S. Eguchi and S. Hironaka et al., Zeolites 18 (1997) 142.

[16] A. Corma, V. Fornes, V. Pergher, Th.L.M. Maesen and J.G. Buglass, Nature 396 (1998) 353.

[17] (a) A. Corma, U. Diaz, M. E. Domine and V. Fornes, J. Am. Chem. Soc. 122 (2000) 2804; (b) A. Corma, U. Diaz, M.E. Domine and V. Fornes, Angew. Chem. Int. Ed. 39 (2000) 1499.

[18] W.M. Meier, D.H. Olson and Ch. Baerlocher, *Atlas of Zeolite Structure Types* (Butterworth, London, 1996) 106–107.

[19] (a) I. Rahmin, A. Huss Jr., N.D. Lissy, J.D. Klocke and O.W. Haag, US Patent 5, 449, 851 (1995); (b) Z.H. Wu, Q.X. Wang, L.Y. Xu and S.J. Xie, Studies Surf. Sci. Catal. 142 (2002) 747.

[20] (a) S.J. Xie, Q.X. Wang, L.Y. Xu, et al., Chin. J. Catal. 20 (1999) 583; (b) S.J. Xie, Q.X. Wang, L.Y. Xu, et al., Chin. J. Catal. 21 (2000) 297; (c) J. Bai, S.L. Liu, S.J. Xie, et al., Catal. Lett. 90 (2003) 123.

[21] H.P. Klug and L.E. Alexander, *X-Ray Diffraction Procedures for Polycrystalline and Amorphous Materials* 2nd edn. (John Wiley & Suns, New York, 1974) 530–550.

[22] R.R. Xu, W.Q. Pang and W.Q. Tu et al., *Zeolite Molecular Sieves Structure and Synthesis* 1st edn. (Jilin University, Jilin, China, 1987) ch.8.

[23] J.B. Peng, S.J. Xie and L.Y. Xu et al., Chin. J. Catal. 23 (2002) 363.

[24] Y.Q. Song, X.X. Zhu and S.J. Xie, Catal. Lett. 97 (2004) 31.

[25] J.Y. Wang, D.Zh. Wang and X.D. Lu, Chin. J. Catal. 14 (1993) 392.

[26] X.Q. Chen, Petrochem. Ind. Trends 7 (1999) 16.

[27] J. Houzvicka, S. Hansildaar and V. Ponec, J. Catal. 167 (1997) 273.

[28] G. Seo, H. Seo and K. Jeong, Catal. Lett. 36 (1996) 249.